Polymer 49 (2008) 4226–4229

Contents lists available at ScienceDirect

Polymer

journal homepage: www.elsevier.com/locate/polymer

Electrospun nanofibers from a porous hollow tube

J.S. Varabhas, G.G. Chase*, D.H. Reneker

Microscale Physiochemical Engineering Center, The University of Akron, Akron, OH 44325-3906, United States

ARTICLE INFO

Article history:
Received 7 April 2008
Received in revised form 18 July 2008
Accepted 26 July 2008
Available online 31 July 2008

Keywords:
Electrospin
Nanofiber
Porous hollow tube

ABSTRACT

Single electrospinning jets are known to have low production rates. A 0.1 m^2 nonwoven mat containing 1 g of 100 nm fibers may take several days to create from a single jet. Inexpensive methods of higher production rates are needed for laboratory research applications. In this paper we present experimental results of many simultaneous electrospinning jets from the surface of tube having a porous wall. The pores in the wall are small and resist the flow of the polymer. Holes drilled half way into the wall of the tube provide points of reduced flow resistance. A polymer solution of 15 wt% polyvinylpyrrolidone (PVP) in ethanol is pushed by low air pressure of 1–2 kPa through the tube wall at the drilled holes. On the outer surface of the tube polymer drops form at the locations of the drilled holes. The solution is charged from 40 to 60 kV to electrospin the polymer. Multiple polymer jets launch from the tube surface and form fibers. A 13 cm long tube with 20 holes can produce 0.3–0.5 g/h of nanofiber. Production rates can easily be scaled by increasing the tube length and the number of holes.

1. Introduction

Many nanofiber applications need large quantities of fiber. The method of electrospinning [1–4] is a convenient method for producing nanofibers but the rate of fiber production is slow. For laboratory research purposes an inexpensive scaleable method with higher production rate is needed. This paper discusses a modification of the porous walled tube described by Dosunmu et al. [5]. In the work by Dosunmu et al. the tube had walls of uniform thickness and uniform flow resistance. The polymer solution passed through the wall and emerged at points randomly distributed over the whole surface of the tube. In this present work small holes are drilled half way through the porous wall to create points of lesser resistance through which the polymer solution preferentially flows. The polymer solution inside the tube is pressurized sufficiently (less than 10 kPa) to force the polymer to flow through the drilled holes but not elsewhere. By controlling the location of the drilled holes one can control the locations at which the electrospinning jets are emitted from the tube wall.

2. Experimental apparatus

In this work a porous hollow tube made of polytetrafluoroethylene (PTFE) (Small Parts Inc., Hollywood, Florida, USA) is used for creating the electrospinning jets. The tube wall has pores with an average pore size in the range of 20–40 μm as shown in Fig. 1. The tube is oriented with its axis horizontal and holes drilled partway into the wall are aligned along the bottom of the tube. The holes are 0.5 mm in diameter and penetrate 1.0 mm into the wall, as shown in the sketch in Fig. 2. The holes are arranged in an array spaced 1 cm apart in two rows parallel to the axis of the tube and the rows are spaced 1 cm apart.

A wire electrode shown in Fig. 3 is inserted inside the tube to maintain an equal electrical potential in the vicinity of each of the drilled holes, even in poorly conducting liquids. The voltage applied to the wire electrode was varied from 40 to 60 kV in our experiments. The wire electrode was made out of a square wire mesh having a 5 mm spacing between the wires. The wire mesh provides high surface area of contact between the wire and the polymer solution inside the tube for uniform charging of the polymer along the length of the tube. The tips of the wires are positioned inside the tube on the inside wall surface closest to the locations of the drilled holes on the outside of the tube wall. The spacing of the wires and the spacing of the drilled holes ensure that a wire tip is not more than 2.5 mm from the axial location of each drilled hole. The wire diameters are approximately 1 mm in diameter and do not interfere with the flow of the polymer mixture.

The porous tube is suspended on a frame of polyvinylchloride (PVC) pipe at adjustable distances of about 12–15 cm above the aluminum foil collector (see Fig. 4). The aluminum foil is grounded to collect the electrospun fibers.

To operate the tube a solution of 15 wt% of polyvinylpyrrolidone (MW 360,000, Sigma–Aldrich, St. Louis, Missouri) in ethanol is loaded into the tube from the 0.8 cm inlet tubes on the top of the

* Corresponding author. Tel.: +1 330 972 7943.
E-mail address: gchase@uakron.edu (G.G. Chase).

0032-3861/$ – see front matter © 2008 Elsevier Ltd. All rights reserved.
doi:10.1016/j.polymer.2008.07.043

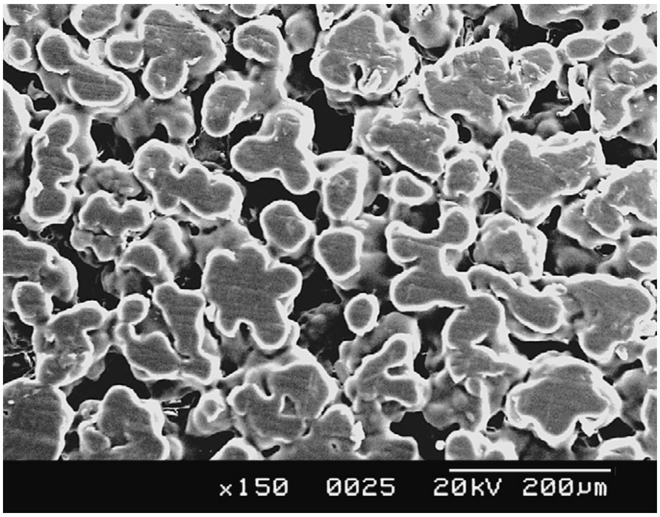

Fig. 1. Scanning electron microscope (SEM) image from surface of porous tube. The dark areas are the open pore channels for the polymer flow. The average pore size is in the range of 20–40 μm.

tube (Fig. 2). The polymer solution was prepared by stirring 15 wt% polyvinylpyrrolidone from Sigma–Aldrich with 85 wt% ethanol as the solvent at room temperature for 12 h.

Air pressure of 1.3 kPa is applied to the top of the tube to push the polymer through the pores and out of the drilled holes. Fig. 5 is a photograph of the tube in operation which shows conical drops of the polymer solution hanging from the bottom of the porous tube at the locations of each of the drilled holes. The polymer jets are present, but not visible against the light background in this figure.

Each hole produces one jet that ultimately forms one long continuous fiber. When the jets reach a distance of a few centimeters from the cones, the electrical bending instability becomes dominant and the jet forms an expanding coil, as shown in Fig. 6. Each segment of the coiled jet moves radially outward and downward [6]. The electrical repulsion between the adjacent jets maintains their separation.

On the left in Fig. 6, glints of steady light reflected from the electrical bending coils form the visible traces shown in the image while approximately 20 turns in the coils move downward through the area shown during the exposure time. On the right, jets from the same three cones are illuminated with a bright strobe light with the steady light turned off. The images of many, but not all,

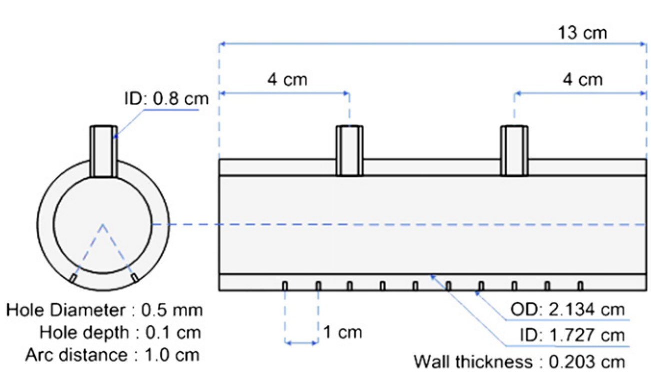

Fig. 2. Cutaway view drawing showing the cylindrical porous hollow tube with its axis oriented horizontally. The left and right ends of the tube are plugged with rubber stoppers. The tube is filled with polymer solution through one of the openings in the top of the tube and air pressure is applied through the openings in the top of the tube to push the polymer solution through the pores in the wall.

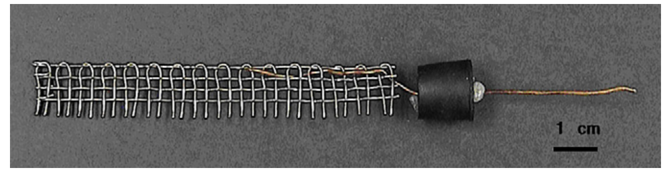

Fig. 3. Photograph of wire electrode inserted inside the tube before filling the tube with polymer solution.

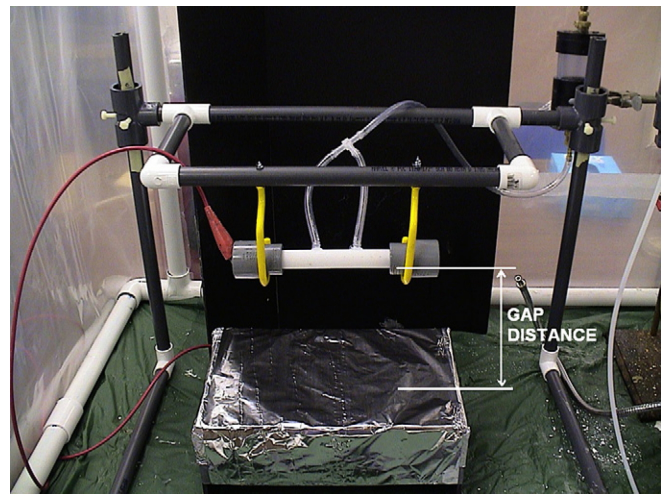

Fig. 4. Framework to hold the porous tube and aluminum foil collector. The gap distance is measured from the bottom of the white tube with end caps to the foil collector.

segments of each coiled jet are recorded during a 35 ms light flash. The segments have a ribbon-like appearance because of their downward motion during the flash.

3. Results and discussion

Experiments were conducted to measure the effects of gap distance and applied voltage on fiber size distribution and production rate. Fiber size distribution was determined by measured diameter and length of fibers in SEM images such as those shown in Fig. 7.

Fiber samples were collected for the same polymer solution for two gap distances (12.7 and 15.4 mm) and three applied voltages (40, 50, and 60 kV).

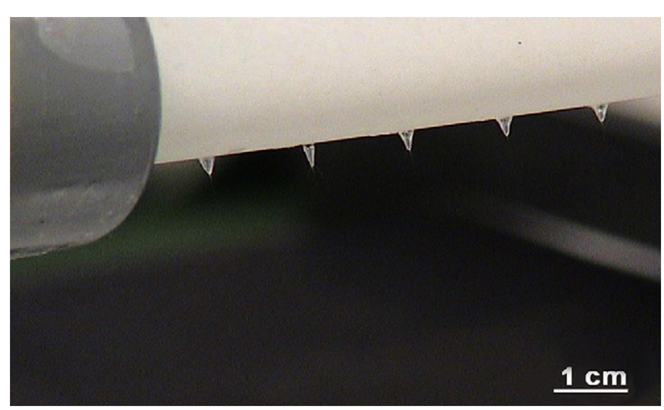

Fig. 5. Close-up photo during electrospinning from the conical drops hanging at the locations of the drilled holes on the porous tube.

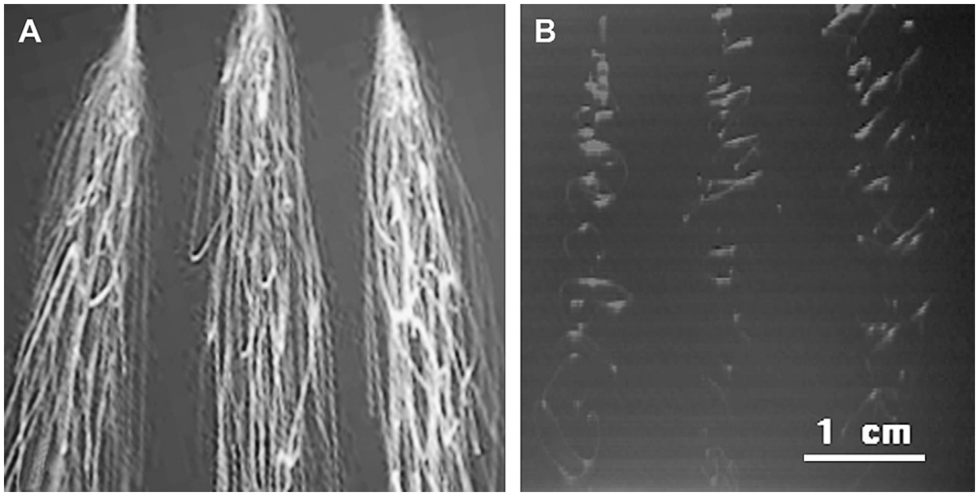

Fig. 6. Photograph of the path of the straight jets launching from the flow modified Taylor cones in Fig. 5. On the left, the jet is illuminated with a steady light and a long exposure time during which many coils pass downward through the region observed. On the right, the same jet was illuminated with a single flash that almost, but not completely, stopped the motion of the segments.

The fiber diameters and lengths were determined using software ImageJ (http://rsb.info.nih.gov/ij/). For each distribution not fewer than 150 fibers from not fewer than 10 SEM images were measured.

The log mean diameters, $\bar{x}_g$ and standard deviations, σ_g, of the log-normal distributions were calculated using the expressions:

$$\ln(\bar{x}_g) = \frac{1}{L_{\mathrm{tot}}}\sum L_i \ln(x_i) \tag{1}$$

$$\ln(\sigma_g) = \sqrt{\frac{\sum\left(L_i(\ln(x_i) - \ln(\bar{x}_g))^2\right)}{L_{\mathrm{tot}}}} \tag{2}$$

where $L_{\mathrm{tot}}=\sum L_i$ and L_i is the length of the fiber segments of diameter x_i. The frequency distributions are determined from:

$$f_i = \frac{1}{d_i}\frac{1}{\ln\sigma_g\sqrt{2\pi}}\exp\left(-\frac{(\ln d_i - \ln \bar{d}_g)^2}{2(\ln\sigma_g)^2}\right) \tag{3}$$

Length weighted log-normal frequency fiber diameter distributions are shown in Fig. 8. The distributions are asymmetric and may be fitted with a log-normal distribution [5]. These results show that the narrowest size distribution and smallest fibers occur with the application of 50 kV for both gap distances. In all cases the average fiber diameters were between 0.3 and 0.6 μm.

To determine the mass production rate the mass of fiber collected on the aluminum foil during a 10 min interval was measured. The result shows that this method can produce fiber in the range of 0.3–0.5 g/h for a 13 cm long tube with 20 holes on the bottom surface of the tube. Electrospinning production rates from a single nozzle (needle or pipette) are typically 0.01–0.1 g/h. This shows that the production rate from the tube is about 3–50 times

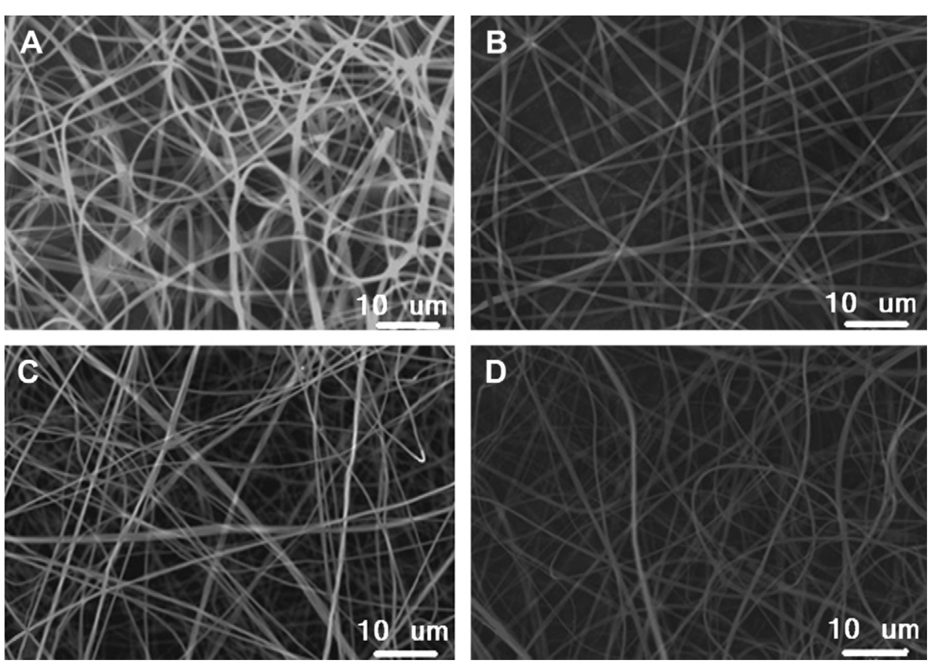

Fig. 7. SEM image of PVP 15 wt% fibers. The upper photos are images of fibers formed with gap distance of 12.7 cm (5 inches) and the lower images for gap distance of 15.2 cm (6 inches). The photos on the left are for 50 kV and on the right for 60 kV applied potentials.

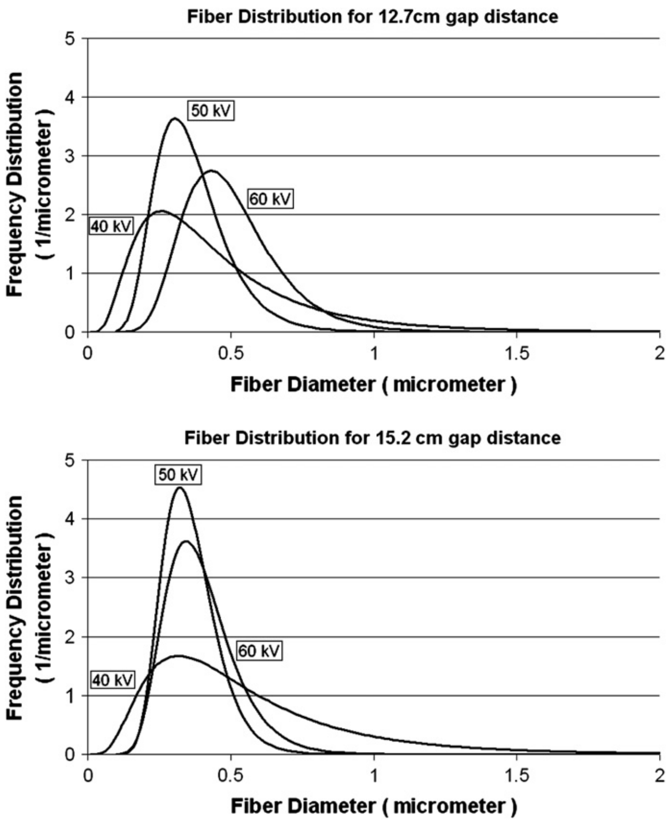

Fig. 8. Length weighted log-normal frequency distribution of fiber diameter of PVP in ethanol from porous tube at different voltages and gap distances.

the rate of that of a single nozzle. The production rate of the tube does not always scale as the number of holes times the single nozzle production rate. The production rate is affected by the spacing between the drilled holes, the number of rows of holes, and external factors such as collector geometry that may affect the strength and uniformity of the potential field that drives the electrospinning process.

Fig. 9 shows an example of fiber mats produced from a porous tube having 20 holes. The white stripes are mats of fibers collected from the jets from each hole. The absence of fibers in the gap between the stripes is consistent with the electric field repulsion between jets shown in Fig. 6. The holes in the tube can be off-set between rows to cause the stripes to overlap as the belt moves and thus create a continuous mat of nanofibers. If the belt moves fast the stripes have fewer fibers than if the belt moves slowly. Multiple tubes could be used to create thicker mats of fibers on a fast moving belt. If the belt is stationary the fibers collect on circular spots. As the mat thickens the collected fibers tend to repel the jet thus making the spot become larger in diameter (as is typical of single jet electrospinning). In this case the spots from the multiple holes become larger and overlap and create a continuous mat as can be seen by the intense white areas in Fig. 9.

Dosunmu et al. [5] showed that the porous tube provides an inexpensive method for producing multiple electrospun jets to increase nanofiber production rates. However, the jets formed randomly around the tube surface and tended to launch in multiple directions with little or no control of the jet direction. The work here shows that the simple modification of the tube walls by partially drilling holes through the wall can effectively control the locations at which drops from and hence control the launching locations of the jets. This gives much greater control over the process and the collection of the electrospun fibers.

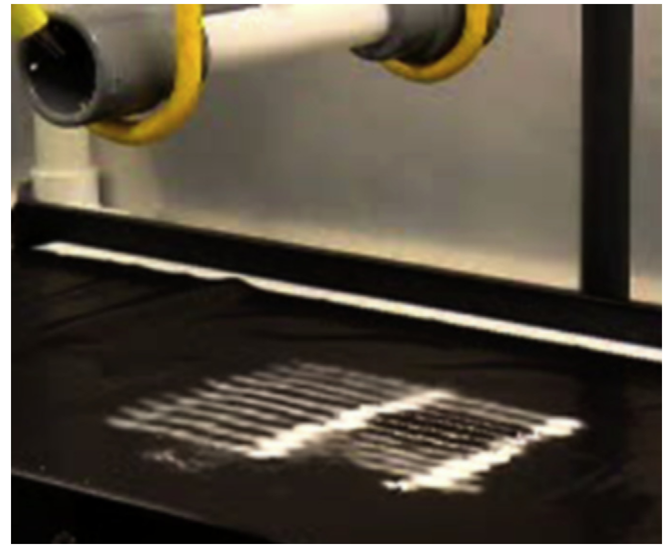

Fig. 9. Photo of nanofibers collected on a moving belt from multiple jets from the porous tube with partial holes. The more intense white areas show where the fiber mats grew in size and overlapped each other when the belt was stationary. The holes in the tube were arranged in two rows of 10 holes each. The row of holes on the right formed the intense white area on the right and the row of holes on the left formed the intense white area on the left. When the belt was put into motion left-to-right the jets formed the white strips shown in the photograph. Between the stripes are dark areas of no fibers or very low concentrations of fibers. The stripes are about 20 cm long and 2 cm wide. The belt had a linear velocity of about 0.4 m/min.

4. Conclusions

We have tested a device for launching multiple jets from a hollow porous cylindrical tube. The device produces fiber mats at mass rates greater than that can be obtained from a single electrospinning jet. The design and setup of the apparatus is relatively simple compared to array of multiple needles. The average fiber diameters produced by this device were in a range of 0.3–0.6 μm.

Acknowledgement

This work supported by the Coalescence Filtration Nanomaterials Consortium: Ahlstrom Paper Group, Donaldson Company, Cummins Filtration, Hollingsworth and Vose, and Parker Hannifin. This work was also supported by the National Science Foundation grant number DMI 0403835.

References

[1] Theron SA, Yarin AL, Zussman E, Kroll E. Polymer 2006;46(9):2889–99.
[2] Reneker DH, Yarin AL, Fong H, Koombhongse S. Journal of Applied Physics 2000;87(9):4531–47.
[3] Theron SA, Zussman E, Yarin AL. Polymer 2004;45(6):2017–30.
[4] Shin YM, Hohman MM, Brenner MP, Rutledge GC. Applied Physics Letters 2001;78(8):1149–51.
[5] Dosunmu OO, Chase GG, Kantaphinan W, Reneker DH. Nanotechnology 2006;17(4):1123–7.
[6] Reneker DH, Yarin AL. Polymer 2008;49(10):2387–425.